Journal of Energetic Materials
Publication details, including instructions for authors and subscription information:
http://www.informaworld.com/smpp/title~content=t713770432

Laser probing and kinetic modeling of NO and CO production in shock-wave decomposition of nitromethane under highly diluted conditions

D. S. Y. Hsu[a]; M. C. Lin[a]
[a] Naval Research Laboratory, Chemistry Division Code 6105, Washington, D.C.

To cite this Article Hsu, D. S. Y. and Lin, M. C.(1985) 'Laser probing and kinetic modeling of NO and CO production in shock-wave decomposition of nitromethane under highly diluted conditions', Journal of Energetic Materials, 3: 2, 95 — 127
To link to this Article: DOI: 10.1080/07370658508012337
URL: http://dx.doi.org/10.1080/07370658508012337

LASER PROBING AND KINETIC MODELING OF NO AND CO PRODUCTION IN SHOCK-WAVE DECOMPOSITION OF NITROMETHANE UNDER HIGHLY DILUTED CONDITIONS

D.S.Y. Hsu and M.C. Lin

Chemistry Division
Code 6105
Naval Research Laboratory
Washington, D.C. 20375-5000

ABSTRACT

The decomposition of nitromethane (CH_3NO_2) in a shock tube has been studied by using a frequency-stabilized CW CO laser to measure the real-time production of NO and CO, two of the key decomposition products. Highly diluted CH_3NO_2/Ar mixtures (0.15 -0.75% CH_3NO_2) were used in incident shock experiments over the temperature range from 940 to 1520K and pressure range from 0.4 to 1.0 atm. A mechanism consisting of 37 chemical reactions was used to model the formation of these two products over the entire range of experimental conditions employed. All but one rate constant (i.e. $CH_3 + CH_2O$) were obtained either from the literature or from simple TST and RRKM calculations. The NO profiles could be quantitatively modeled over the entire temperature range, whereas those of CO could be accounted for only by increasing the values of the rate constant for $CH_3 + CH_2O$ determined at low temperatures by more than a factor of 30. The reason for this adjustment is discussed. The combination of the evaluated rate constants with others for the $CH_3 + CH_2O$ reaction covering the range of 350-1500K gave rise to the expression:

$$k_{20} = 6.6 \times 10^{-38}\ T^{15.43}\ e^{+4320/T}\ \text{cc/mole·sec}$$

Additionally, strong oscillatory behavior in the NO and CO profiles was observed when 2.5 - 3.0% CH_3NO_2 mixtures were shock-dissociated. A similar behavior was not detected in CH_3ONO decomposition under the same conditions. The comparison of these two isomeric systems will be made.

Journal of Energetic Materials vol. 3, 95-127 (1985)

Published in 1985 by Dowden, Brodman & Devine, Inc.

INTRODUCTION

There have been numerous early studies on the thermal decomposition of nitromethane,[1-6] with the majority of the experiments carried out below 1000 K using pure CH_3NO_2. Because of the complexity of the reactions involved, it was rather difficult to determine accurately the rate for the initial dissociation process and the mechanism for the overall decomposition reaction. Glänzer and Troe[7] investigated the decomposition reaction in a shock tube using highly diluted CH_3NO_2. The disappearance of CH_3NO_2 and the appearance of NO_2 were monitored spectroscopically in the UV and visible regions, respectively. The rate constants for the initiation process,

$$CH_3NO_2 \rightarrow CH_3 + NO_2$$

were measured over a broad range of temperature and pressure, and the values for the unimolecular dissociation reaction at the high and low pressure limits were reliably determined for the first time.[7] More recently, Perche and co-workers[8] studied the decomposition reaction under low pressure and low temperature conditions in an attempt to establish the mechanism for the overall decomposition reaction. A mechanism consisting

of some 30 reactions was employed to simulate the formation of various products (for example, CH_2O, HCN, CH_3OH, CH_4, H_2O, NO_x, CO_x, N_2O and N_2) measured by GC analysis and/or UV absorption. Reasonable, semiquantitative agreement between observed and calculated profiles could be achieved by judicious choices of rate constants for the selected reactions.[8]

In this experiment we employed a shock tube, in conjunction with a stabilized CW CO laser, to study the kinetics of production of NO and CO, two of the key products of CH_3NO_2 decomposition at high temperatures. Our objective lies in the establishment of a reasonable mechanism for simulation of these two chemically active intermediates, which undoubtedly play important roles in the ultimate energy release from the ignition or detonation of CH_3NO_2 under high temperature and pressure conditions.

EXPERIMENTAL

The details of the shock tube and the frequency-stabilized CW CO probe laser were given in previous publications[9,10]. In this work incident shocks were used because of the high reactivity of the primary

decomposition products. For the NO absorption measurements, the 7 → 6 P(13) transition of the CO laser was used, thanks to its near coincidence with the $^2\pi_{3/2}$ v = 0 → 1, J = 37/2 → 39/2 transition in NO.[10-12] For the CO absorption measurements, the 2 → 1 P(10) CO laser line was used, instead of the more sensitive 1 → 0 transition, because of its easiness to be stabilized. All calculations for post-shock gas properties such as temperature, pressure and density were made by using the NASA/LEWIS equilibrium program.[13] Spectral grade nitromethane (Aldrich Chemical Co.) and ultra-high purity Ar (99.999% Matheson Gas Products) were used for the reaction mixtures.

NO and CO Absorption Calibrations

To obtain the NO absorption coefficients for our experimental conditions, we used the line strength S and the mean line-shape function ϕ from the careful work by Hanson, Monat and Kruger,[11] who calibrated the near-coincident NO absorption of the 7 → 6 P(13) (CO laser line at 1935.4817 cm^{-1}. These two quantities allowed us to calculate the NO absorption coefficient $\alpha = S\phi$ for this CO laser line at any temperature and pressure under our experimental conditions. To check the

validity of α, we shocked 1 and 2% mixtures of NO in Ar over the temperature range of 715-2185K and pressure range of 0.6-1.9 atm. and measured the NO absorption of the 7 → 6 P(13) CO laser line. A maximum average deviation of only 3% was found between the calculated and experimental NO pressure over the entire temperature range employed[10,12]. The details on the calculations and testing of the NO absorption coefficient can be found in the paper by Hanson, Monat and Kruger,[11] and in our earlier paper on methyl nitrite decomposition.[12]

The calibration of CO resonance absorption of CO laser lines was carried out in this laboratory and was discussed in an earlier paper.[9] Briefly, known dilute CO/Ar mixtures were shocked over a wide range of temperature and pressures (0.36-1.42% CO in Ar, 1.6-4.8 atm., 1550-3260 K). The CO absorption measurements were taken with the CO laser operating in the 2 → 1 P(10) transition.

By determining the only unknown quantity, the Lorentz half-width at room temperature, $\gamma^{\circ} = 0.0522 \pm 0.0021$ cm^{-1} atm^{-1} in the gain equation, absolute CO concentrations could be calculated from the laser absorption data obtained under wide ranges of temperatures and pressures.[9,10]

RESULTS AND DISCUSSION

Decomposition of Nitromethane Under Highly Diluted Conditions

In order to minimize complication due to secondary and tertiary reactions, most of our experiments were carried out using highly diluted CH_3NO_2. Incident shock experiments using mixtures with 0.15, 0.25, 0.40, and 0.76% CH_3NO_2 in Ar were carried out over the temperature range 940-1520K and pressure range 0.4-1.0 atm. NO absorption measurements were taken for all four mixtures with the CO laser operating on the 7 → 6 P(13) transition, and the CO data were taken for the last three mixtures with the laser operating on the 2 → 1 P(10) line. The absorption data were converted into absolute NO and CO concentration - time profiles by the aforementioned calibrated absorption coefficients. Typical NO and CO concentration-time profiles at different temperatures are shown respectively by the triangles and circles in Figures 1, 2, and 3. The time scales shown have been converted to the "particle frame".

Kinetic Modeling of NO and CO Formation

The measured NO and CO formation profiles over the

entire range of temperature and pressure studies have been modeled with the CHEMEQ kinetics program[14] using a mechanism consisting of 37 reactions listed in Table 1. This mechanism was based primarily on that of Perche et al.[8] and the presently well-established mechanism of CH_4 oxidation reaction at high temperatures[18]. All except 10 of the rate constants given in Table 1 were well accepted in the literature. The appropriate values of the initiation rate constant for the pressure and temperature range of our experiments were taken from the work of Glänzer and Troe.[7] Those less well-established rate constants under the conditions employed were extrapolated or re-evaluated by means of the simple transition-state theory (TST, for direct metathetical processes) and the Rice-Ramsperger-Kassel-Marcus theory (RRKM,for unimolecular and bimolecular processes that occur via long-lived intermediates)[18] as noted in the table. The calculated rate constants were fitted by least squares to the equation of the form: $k = AT^B\exp(-E_a/RT)$. For two of the five reactions calculated with the RRKM theory, i.e. Reactions (14) and (16), the computed rate constants were found to be pressure-independent and their original source values were used.

The profiles of NO production could be quantitatively simulated over the whole range of temperature and pressure studied with essentially no adjustment of the rate constants adopted. The solid curves given in Figures 1-3 represent the calculated typical NO profiles for low, medium and high temperature runs.

The profiles of CO production, on the other hand, could not be satisfactorily accounted for without readjusting the value of the rate constant for the reaction, $CH_3 + CH_2O \rightarrow CH_4 + CHO$, which was identified as the most important CO rate-controlling reaction aside from the initiation process through sensitivity analysis (to be discussed below). A reasonable fitting of all measured CO production profiles could be obtained if the rate constant for $CH_3 + CH_2O$ took on a value of $\sim 10^{12}$ cm^3/mole.sec. without varying other rate constants. Table 2 lists the experimental conditions of the runs which have been modeled and the values of k_{20} for $CH_3 + CH_2O$ derived from the modeling of those runs for which CO production profiles have been measured. Further discussion on reaction (20) is made in the appendix.

The sensitivity analysis alluded to above was performed for each reaction included in Table 1 to gauge its importance for NO or CO production. For the typical

experimental conditions of 1243K, 0.70 atm. and 0.76% CH_3NO_2 mole fraction (corresponding to the runs shown in Figure 2), the rate constant of each reaction was doubled and then halved and the percent changes in the NO and CO concentrations at t = 60 μs were noted. Both NO and CO concentrations were increasing rapidly at t = 60 μs, which should be a responsive time for the sensitivity test. The results which indicated 3% or more change were listed at the right side in Table 1. Aside from the obvious high sensitivity of the initiation reaction to both NO and CO production, it is worth noting that relatively few remaining reactions are sensitive toward NO production. Among these, are $CH_3 + NO_2 \rightarrow CH_3O + NO$ and $CH_3 + CH_3 \rightarrow C_2H_6$; both are fairly well-established processes.

For CO production, the remaining influential reactions (aside from the initiation process) are given in declining order:

$$CH_3 + CH_2O \rightarrow HCO + CH_4 \quad (20)$$

$$CH_3 + CH_3 \rightarrow C_2H_6 \quad (31)$$

$$CH_3 + NO_2 \rightarrow CH_3O + NO \quad (3)$$

$$CH_2O + OH \rightarrow HCO + H_2O \quad (19)$$

$$CH_2O + H \rightarrow HCO + H_2 \quad (18)$$

$$CH_3NO_2 + OH \rightarrow CH_2NO_2 + H_2O \quad (13)$$

As it has been clearly demonstrated in the CO modeling in our earlier paper,[18] CO production depends solely on the production of CH_2O and its reactions with radicals to form HCO leading to CO. On this basis the sensitivity of Reactions (20), (31), (3), (19), (18) and (13) to CO production becomes quite evident. It should be noted that Reaction (13) has a negative effect on CO production. In fact, omitting Reaction (13) altogether from the scheme increased the CO concentration at 60 μs by 47%. This effect may be caused by the fact that Reaction (13) slows the chain Reactions (19), (25) and (8) involving H and OH radicals by consuming OH without yielding H atoms to regenerate more OH through Reaction (8), $NO_2 + H \rightarrow NO + OH$. Whereas the reactions of CH_2O with OH generate more H atoms to sustain the chain reaction. This modeling exercise elucidates the following major progress pattern of our reaction scheme:

(1) Cleavage of the NO_2 group from CH_3NO_2

(2) The major portion of NO is formed early on from Reaction (3), $CH_3 + NO_2 \rightarrow CH_3O + NO$

(3) The dominant routes of formation of CH_2O, the precursor of CO, are Reaction (4), $CH_3O + M \rightarrow CH_2O + H + M$, and Reactions (12), (13) and (14) involving H and OH reactions with CH_3NO_2 leading

first to CH_2NO_2 which unimolecularly decomposes to CH_2O.

(4) Although the CH_3NO_2 + OH contributes significantly to CH_2O production, it tends to slow down the early rate of CO formation by diverting the OH radicals from the chain reaction with CH_2O.

(5) CO formation takes place through the reactions of CH_2O with CH_3, OH, and H radicals.

(6) C_2H_6 formation and the subsequent C-2 chemistry slow down the CO formation.

Comparison of the CH_3NO_2 and CH_3ONO Systems

Nitromethane and methyl nitrite are geometric isomers with similar energy contents. Both compounds can theoretically decompose into CH_3 and NO_2 with similar enthalpy changes. Methyl nitrite, on the other hand, can dissociate much more readily via another substantially lower energy path, producing CH_3O and NO, which is not available to nitromethane; viz.

$$CH_3NO_2 \rightarrow CH_3 + NO_2, \quad \Delta H^\circ = 60.1 \text{ kcal/mole}$$

$$CH_3ONO \rightarrow CH_3 + NO_2, \quad \Delta H^\circ = 57.8 \text{ kcal/mole}$$

$$\rightarrow CH_3O + NO, \quad \Delta H^\circ = 40.7 \text{ kcal/mole}$$

In our recent study of CH_3ONO decomposition[12] in shock waves (680K < T < 955K) we have demonstrated that the NO formed in the reaction remains essentially unreactive and the chain reactions generated by the breakdown of CH_3O involve mainly H atoms with very little contribution from OH radicals. This is illustrated in Figure 4 by the calculated concentration profiles of various key species formed in CH_3ONO pyrolysis at 1050K for a 0.25% CH_3ONO-Ar mixture at a total pressure of 0.83 atm.

The decomposition of CH_3NO_2 under the same reaction conditions, however, is far more complex. Although the initial breakdown of CH_3NO_2 is relatively slow at 1050K, CH_3, H and OH radicals all come into play in the very early stage of the pyrolysis (see Figure 5).

The most obvious difference between these two isomeric systems is the relative abundance of H and OH: in CH_3ONO, $[H] \approx 10^6[OH]$, whereas in CH_3NO_2, $[H] \approx [OH]$. The OH concentration in the latter system is over 10^3 times more abundant than in the former. This is important because the reactions of OH radicals with the parent molecules and CH_2O, the key chain carrier in both systems, are much faster and more exothermic than the corresponding reactions of atoms. Additionally, the OH

radical in the CH_3NO_2 system, on the basis of this modeling, is generated by one of the fastest and exothermic gas phase reactions, H + NO_2, which is nonexistent in the CH_3ONO system.

This major difference is most vividly manifested by the appearance of oscillatory behavior shown in Figure 6 in the NO and CO absorption traces observed in the decomposition of CH_3NO_2 at a concentration as low as 3%. This behavior was not detected in the experiments using CH_3ONO under similar conditions. This finding can be readily rationalized by the occurrence of those rapid, exothermic reactions involving H and OH in the CH_3NO_2 system. This type of oscillation induced by spinning detonations[34] has been seen previously in several exothermic systems.[35] The ignition behavior of high concentration (~10 - 100%) CH_3NO_2 mixtures has been investigated recently in this laboratory.[36]

CONCLUSIONS

The decomposition of highly diluted nitromethane in argon has been studied in a shock tube using a frequency-stabilized CW CO laser to measure the absolute concentration-time profiles of the NO and CO products.

The NO production could be modeled quite successfully throughout the temperature range studied (940 -1520K) with no adjustment to the adopted rate constants in the kinetic scheme. This reflects that our NO data are in close accordance with the initiation rate constant measured by Glänger and Troe. The CO formation could also be modeled successfully provided that we make the only adjustment in the rate constant for the $CH_3 + CH_2O \rightarrow CHO + CH_4$ reaction, for which the rate constant in the temperature range of interest had not been previously measured. The rationale behind this adjustment has been given.

Our kinetic scheme of 37 reactions, including 9 less well studied reactions for which we carried out TST and RRKM calculations, seems to adequately describe the real-time production of NO and CO under the conditions employed. In the view that NO is an early product and CO a late product, our kinetic scheme serves well as a starting point for the modeling of the CH_3NO_2 decomposition system under high-concentration conditions.

APPENDIX

Further Comments on $CH_3 + CH_2O$

The rate constants for the reaction of CH_3 with CH_2O producing CH_4:

$$CH_3 + CH_2O \rightarrow CH_4 + CHO \qquad [20]$$

have been measured by Kutschke and co-workers[37] covering 360-460K using different sources of CH_3 radicals. The recommended rate constant[38]

$$k_{20} = 10^{11.02 \pm 0.6} \exp(-3050 \pm 500/T) cm^3/mole.sec$$

was based primarily on the two sets of data obtained by Kutschke and co-workers. These data and the fitted TST result are presented in Figure A together with the modeled values at high temperatures. As indicated, our high temperature results are larger than the TST-extrapolated values by more than a factor of 30 above 1000K. Very interestingly, however, our values seem to be in line with those reported by Pacey and coworkers[39,40] obtained at temperatures between 800 and 1000K and those of Aronowitz and Naegeli,[41] obtained at 1063 to 1223K. A nonlinear least-squares fit of all experimental points covering 350-1500K led to the expression:

$$k_{20} = 6.6 \times 10^{-38} T^{15.43} e^{+4320/T} \text{ cc/mole·sec}$$

The apparent sharp increase in the rate constant at high temperatures, aside from possible uncertainties

in the kinetic modeling due to compounded errors in the other rate constants used, may be attributed to the following two possibilities which were found to occur in the analogous CH_3 + CH_3CHO reaction:[42]

(1) The occurrence of quantum-mechanical tunnelling which causes a much faster upturn in the rate constant at higher temperatures;

(2) The occurrence of a new reaction channel at higher temperatures:

$CH_3 + CH_2O \rightarrow CH_3CHO + H$, $\Delta H^\circ = 4.0$ kcal/mole

which can generate new chain processes effectively contributing more CO production. For CH_3 + CH_3CHO, the production of CH_3COCH_3 + H has been observed experimentally.[42]

In view of the importance of this process in high temperature hydrocarbon combustion chemisty, a direct measurement for the rate constant above 1000K will be worthwhile.

Acknowledgement

The authors are grateful to Mr. G.L. Burks for carrying out some of the high concentration CH_3NO_2 experiments.

TABLE 1

Reactions and Rate Constants[a] Used in Modeling NO and CO Formed in CH_3NO_2 Decomposition

	Reaction	A	B	E_a	Ref	Sensitivity %[NO] 2 k	Sensitivity Change k/2	Sensitivity %[CO] 2 k	Sensitivity Change k/2
(1)	$CH_3NO_2 + M \rightarrow CH_3 + NO_2 + M$	6.0×10^{16}	0.0	44.0	7	+ 55	- 46	+ 117	- 63
(2)	$CH_3 + NO_2 + M \rightarrow CH_3NO_2 + M$	1.2×10^{14}	0.0	-12.6	b				
(3)	$CH_3 + NO_2 \rightarrow CH_3O + NO$	1.3×10^{13}	0.0	0.0	7	+ 7	- 12	+ 12	- 16
(4)	$CH_3O + M \rightarrow CH_2O + H + M$	4.0×10^{40}	-7.5	22.6	15				
(5)	$CH_3O + NO_2 \rightarrow CH_2O + HONO$	4.0×10^{11}	0.0	0.0	16				
(6)	$CH_3O + NO \rightarrow CH_2O + HNO$	3.2×10^{12}	0.0	0.0	16				
(7)	$CH_3O + OH \rightarrow CH_2O + H_2O$	3.2×10^{13}	0.0	0.0	15				
(8)	$NO_2 + H \rightarrow NO + OH$	2.9×10^{14}	0.0	0.81	16	0	- 1	- 3	+ 3
(9)	$CH_3 + OH \rightarrow CH_2O + H_2$	8.0×10^{12}	0.0	0.0	17				
(10)	$CH_3 + OH \rightarrow CH_3O + H$	2.0×10^{16}	0.0	27.4	17				

TABLE 1
Reactions and Rate Constants[a] Used in Modeling
NO and CO Formed in CH_3NO_2 Decomposition
(continued)

Reaction	A	B	E_a	Ref	Sensitivity %|NO| 2 k	Change k/2	%|CO| 2 k	Change k/2
(11) $CH_3NO_2 + CH_3 \rightarrow CH_2NO_2 + CH_4$	2.4×10^{11}	0.0	9.0	8				
(12) $CH_3NO_2 + H \rightarrow CH_2NO_2 + H_2$	2.5×10^{9}	1.27	2.64	(18,C)	0	0	- 3	+ 2
(13) $CH_3NO_2 + OH \rightarrow CH_2NO_2 + H_2O$	1.7×10^{4}	2.48	-2.42	(TST, this work,[d])	+ 3	- 2	- 6	+ 5
(14) $CH_2NO_2 \rightarrow CH_2O + NO$	1.0×10^{13}	0.0	36.0	RRKM, 19				
(15) $CH_3 + NO + M \rightarrow CH_3NO + M$	8.2×10^{31}	-5.24	3.78	RRKM, 20				
(16) $CH_3NO \rightarrow HCN + H_2O$	7.9×10^{12}	0.0	39.3	RRKM, 22				
(17) $CH_3NO + M \rightarrow CH_3 + NO + M$	7.5×10^{40}	-6.85	48.4	RRKM, 20				
(18) $CH_2O + H \rightarrow HCO + H_2$	2.5×10^{9}	1.27	2.64	TST,18	- 1	0	+ 9	- 5
(19) $CH_2O + OH \rightarrow HCO + H_2O$	6.9×10^{4}	2.65	-1.9	TST,18	- 1	0	+ 13	- 9
(20) $CH_2O + CH_3 \rightarrow HCO + CH_4$	1.0×10^{12}	to fit CO			+ 2	- 2	+ 35	- 27

TABLE 1

Reactions and Rate Constants[a] Used in Modeling
NO and CO Formed in CH_3NO_2 Decomposition

(continued)

Reaction	A	B	E_a	Ref	Sensitivity %[NO] 2 k	Sensitivity %[NO] Change k/2	Sensitivity %[CO] 2 k	Sensitivity %[CO] Change k/2
(21) HNO + M → H + NO + M	2.9×10^{16}	0.0	48.8	24				
(22) H_2 + OH → H_2O + H	5.2×10^{13}	0.0	6.5	25				
(23) H_2O + H → H_2 + OH	2.2×10^{14}	0.0	21.8	b				
(24) HONO + M → NO + OH + M	1.8×10^{30}	-3.86	52.3	RRKM				
(25) HCO + M → CO + H + M	1.6×10^{14}	0.0	14.7	26	+ 2	- 3	+ 2	- 4
(26) HCO + NO_2 → HONO + CO	1.0×10^{14}	0.0	0.0	16				
(27) HCO + NO → HNO + CO	2.0×10^{11}	0.5	2.0	15				
(28) CO + OH → H + CO_2	6.3×10^{7}	1.3	-0.765	27				
(29) CO + NO_2 → NO + CO_2	1.9×10^{12}	0.0	29.3	15				
(30) CH_3O + CH_3O → CH_3OH + CH_2O	1.1×10^{13}	0.0	0.0	16				

TABLE I

Reactions and Rate Constants[a] Used in Modeling
NO and CO Formed in CH_3NO_2 Decomposition

(continued)

Reaction	A	B	E_a	Ref	Sensitivity %[NO] 2 k	Change k/2	%[CO] 2 k	Change k/2
(31) $CH_3 + CH_3 \rightarrow C_2H_6$	3.0×10^{12}	0.0	0.0	28,e	- 6	+4	-18	+15
(32) $CH_3 + C_2H_6 \rightarrow CH_4 + C_2H_5$	5.5×10^{14}	0.0	21.5	29				
(33) $C_2H_6 + OH \rightarrow H_2O + C_2H_5$	6.3×10^{13}	0.0	3.6	30				
(34) $C_2H_5 + M \rightarrow H + C_2H_4 + M$	4.7×10^{14}	0.0	26.6	31				
(35) $C_2H_5 + NO_2 \rightarrow CH_3 + CH_2O + NO$	1.3×10^{13}	0.0	0.0	32				
(36) $C_2H_4 + OH \rightarrow CH_2O + CH_3$	5.0×10^{12}	0.0	0.0	33				
(37) $CH_4 + OH \rightarrow CH_3 + H_2O$	3.2×10^{13}	0.0	5.0	15				

[a] In cc, mole, s units, in form $k = AT^B \exp(-E_a/RT)$
[b] Obtained from equilibrium constant and the forward rate constant.
[c] Taken to be same as those calculate for CH_2O reaction using TST.
[d] Based on the rate constant measured by S. Zabarnick, J.W. Fleming, and M.C. Lin (to be published).
[e] Recombation rate constant depends on M(Ar) concentration. The value shown is for 1243K at 0.70 atm.

TABLE 2

Experimental Conditions of Successfully Modeled NO and CO Profiles

CH_3NO_2 molefraction (%)	NO[a] T(K)	P(atm)	CO T(k)	P(atm)	k_{20}(cm^3/mole·sec)[b]
0.76	943	0.90	1196	0.61	$1x10^{12}$
0.76	1051	0.83	1236	0.65	$1x10^{12}$
0.76	1087	0.87	1266	0.61	$1.5x10^{12}$
0.76	1095	0.81			
0.76	1095	0.66			
0.76	1114	0.67			
0.76	1163	0.79			
0.76	1243	0.70			
0.76	1297	0.63			
0.76	1346	0.58			
0.40	1035	0.87	1147	0.77	$5x10^{11}$
0.40	1064	0.84	1211	0.75	$1x10^{12}$
0.40	1089	0.79	1224	0.68	$3x10^{12}$
0.40	1113	0.59	1299	0.64	$5x10^{12}$
0.40	1130	0.68	1380	0.59	$5x10^{11}$
0.40	1131	0.77			
0.40	1243	0.69			
0.40	1304	0.64			
0.40	1342	0.57			
0.40	1392	0.59			
0.40	1518	0.55			

TABLE 2

Experimental Conditions of Successfully Modeled NO and CO Profiles

CH_3NO_2 molefraction (%)	NO[a] (T(K)	P(atm)	CO T(k)	P(atm)	k_{20}(cm^3/mole.sec)[b]
0.25	1020	0.86	1057	0.83	1.5×10^{12}
0.25	1051	0.83	1080	0.79	1.5×10^{12}
0.25	1123	0.76	1285	0.63	8×10^{11}
0.25	1163	0.72	1344	0.57	2×10^{12}
0.25	1215	0.67	1511	0.55	8×10^{12}
0.25	1295	0.64			
0.25	1304	0.64			
0.25	1332	0.58			
0.15	1029	0.87			
0.15	1059	0.83			
0.15	1138	0.77			
0.15	1253	0.69			
0.15	1297	0.63			
0.15	1355	0.77			
0.15	1376	0.59			
0.15	1384	0.59			

a k_{20} was fixed at 1×10^{12} cm^3/mole.sec in the modeling of the NO profiles.

b Only rate constant adjusted in kinetic scheme to fit the CO profiles.

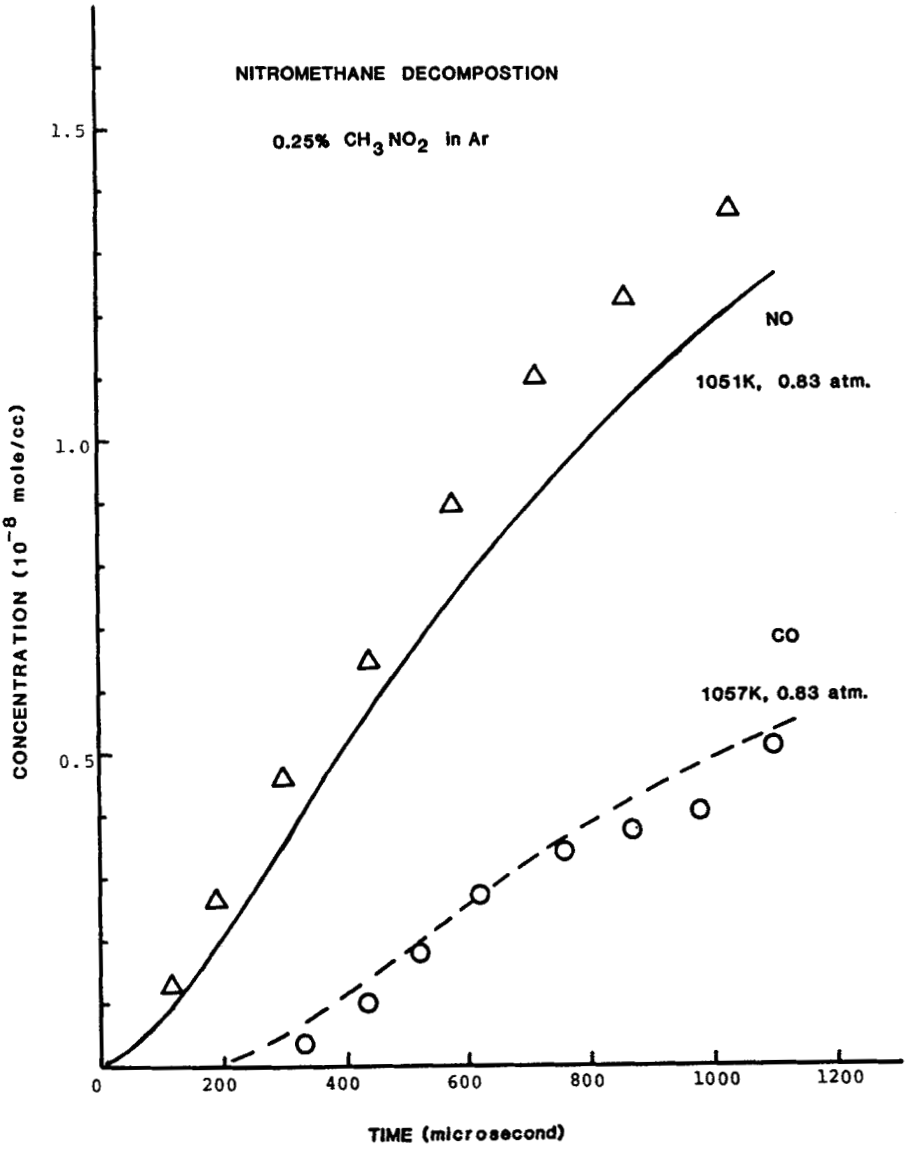

FIGURE 1

Typical NO (triangles) and CO (circles) concentration-time profile data and kinetic-modeled results (dashed and solid curves) for a 0.25% CH_3NO_2/Ar mixture at similar post-shock temperatures and pressures (~1050 K and 0.8 atm.)

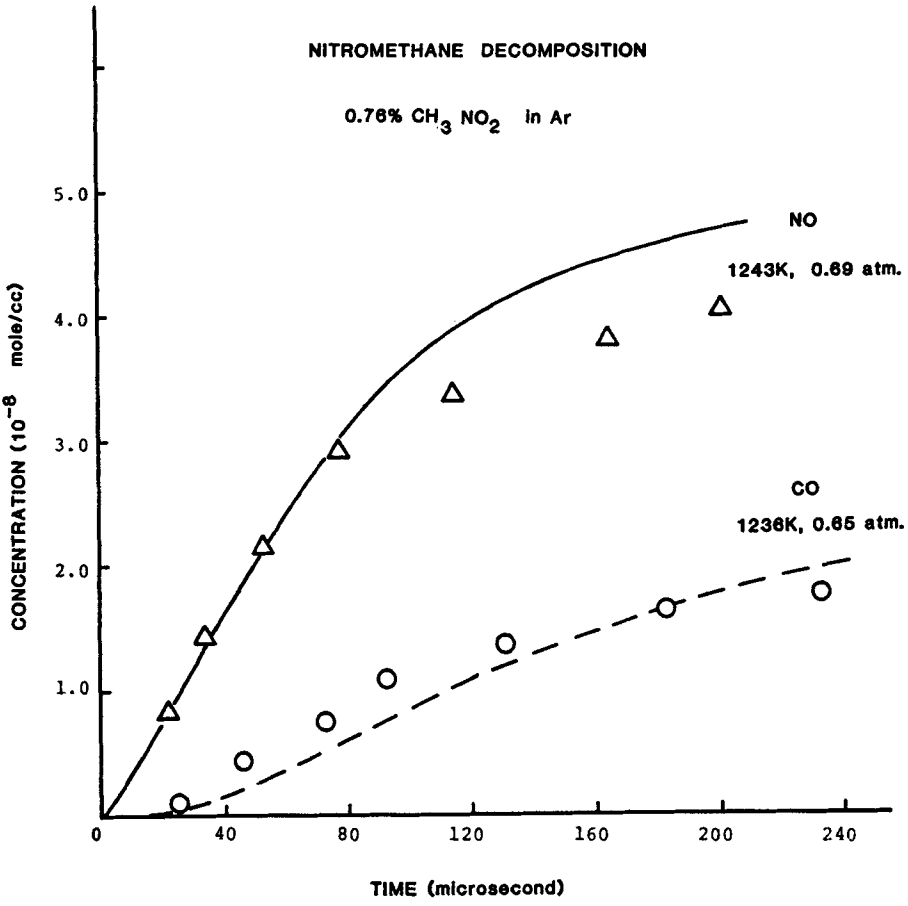

FIGURE 2

Typical NO and CO experimental and modeled results for a 0.76% CH_3NO_2/Ar mixture at ~1240K and 0.7 atm.

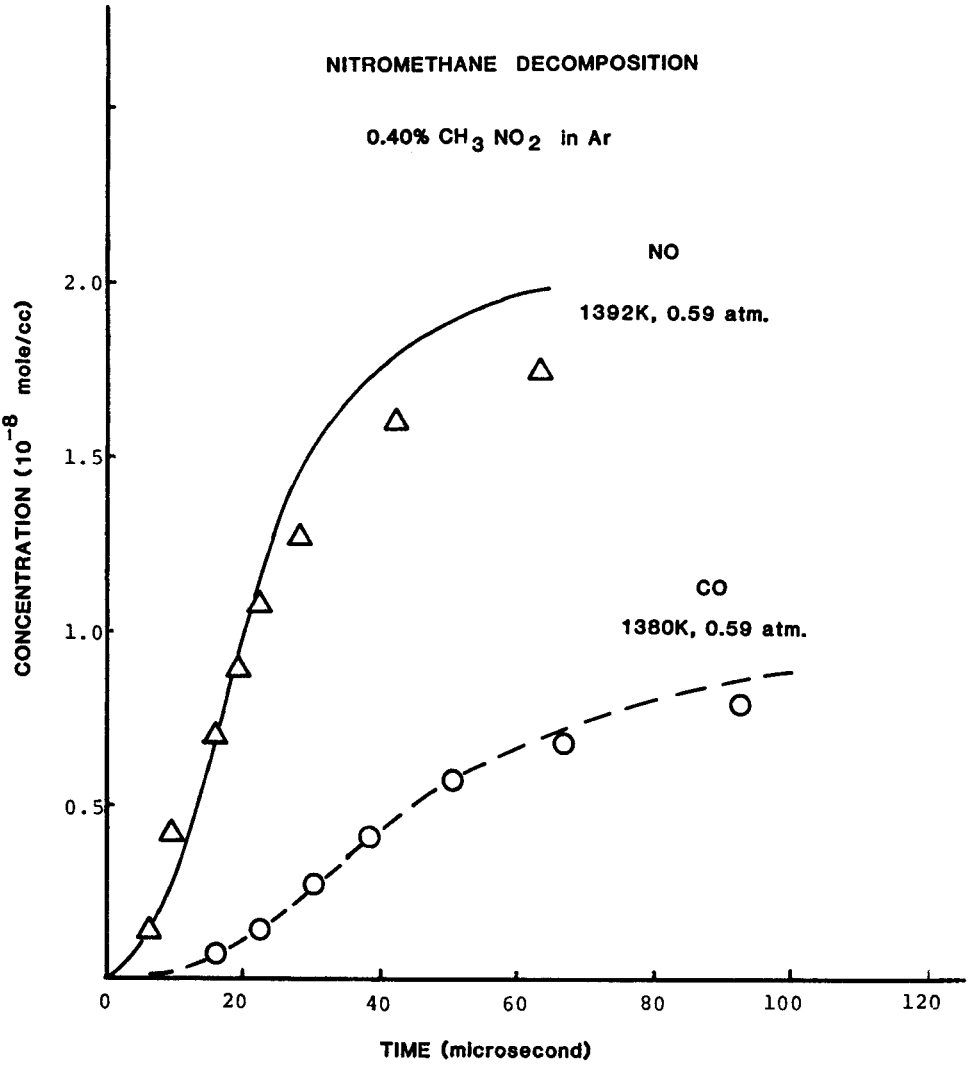

FIGURE 3

Typical NO and CO experimental and modeled results for a 0.40% CH_3NO_2/Ar mixture at ~1380K and 0.6 atm.

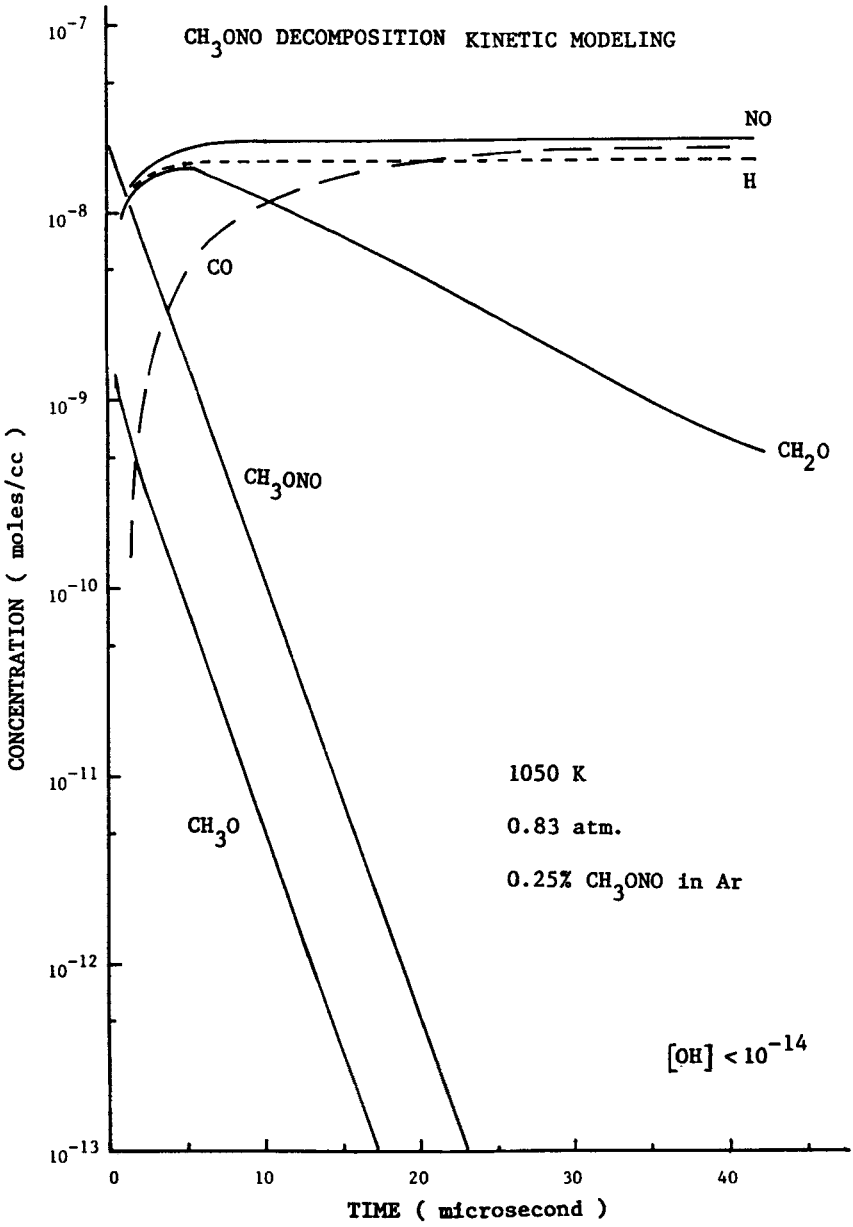

FIGURE 4

Calculated concentration-time profiles of important species in methyl nitrite decomposition under conditions of 0.25% CH_3ONO/Ar, 1050K and 0.83 atm.

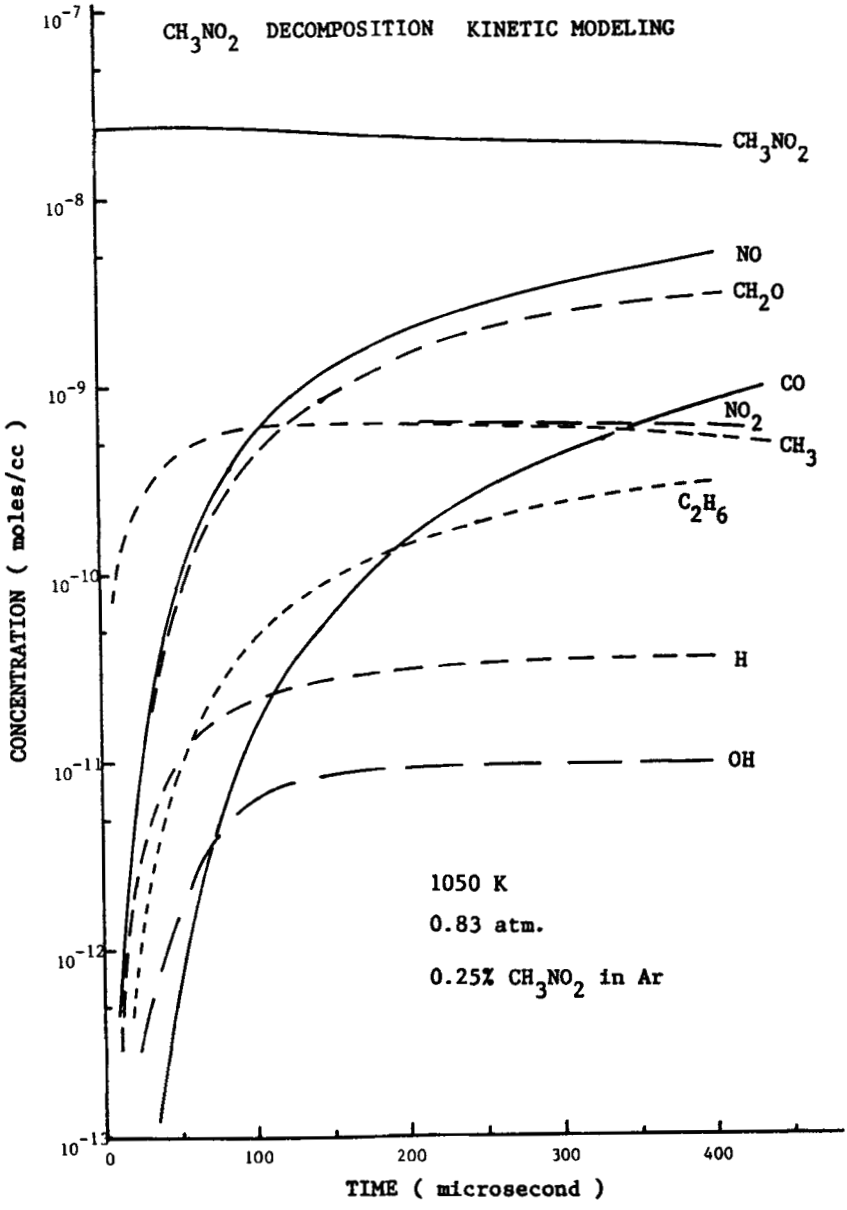

FIGURE 5

Calculated species profiles in nitromethane decomposition under same conditions as Figure 4.

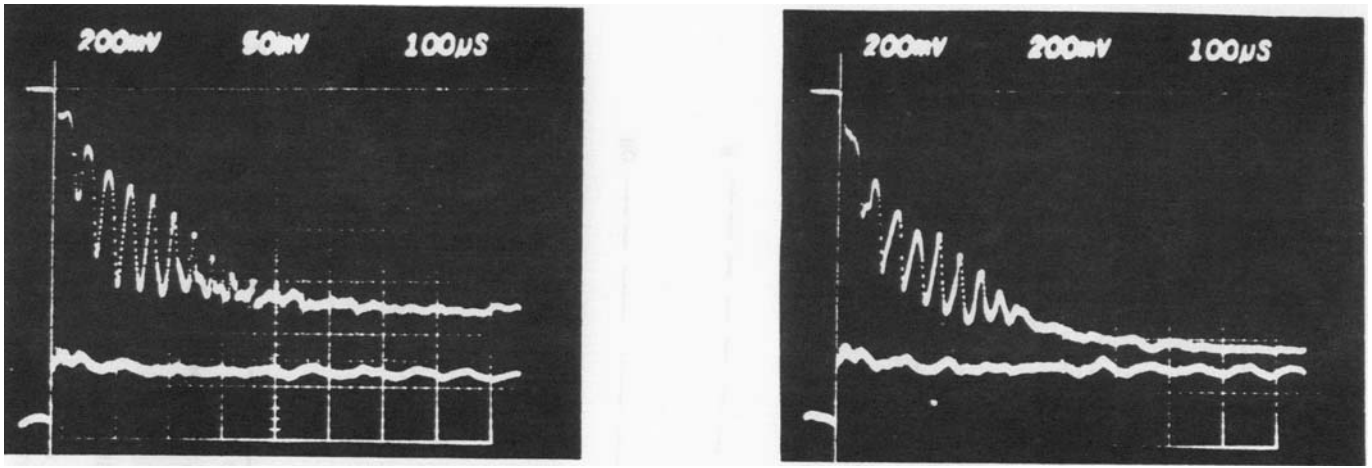

CO absorption
1158 K
0.703 atm
2.9% CH_3NO_2 in Ar

NO absorption
1140 K
0.689 atm
3.1% CH_3NO_2 in Ar

FIGURE 6

Typical CO and NO absorption traces showing oscillations observed for 3% CH_3NO_2 in Ar. The lower traces are pressure traces. The time scale is 100 μs/div.

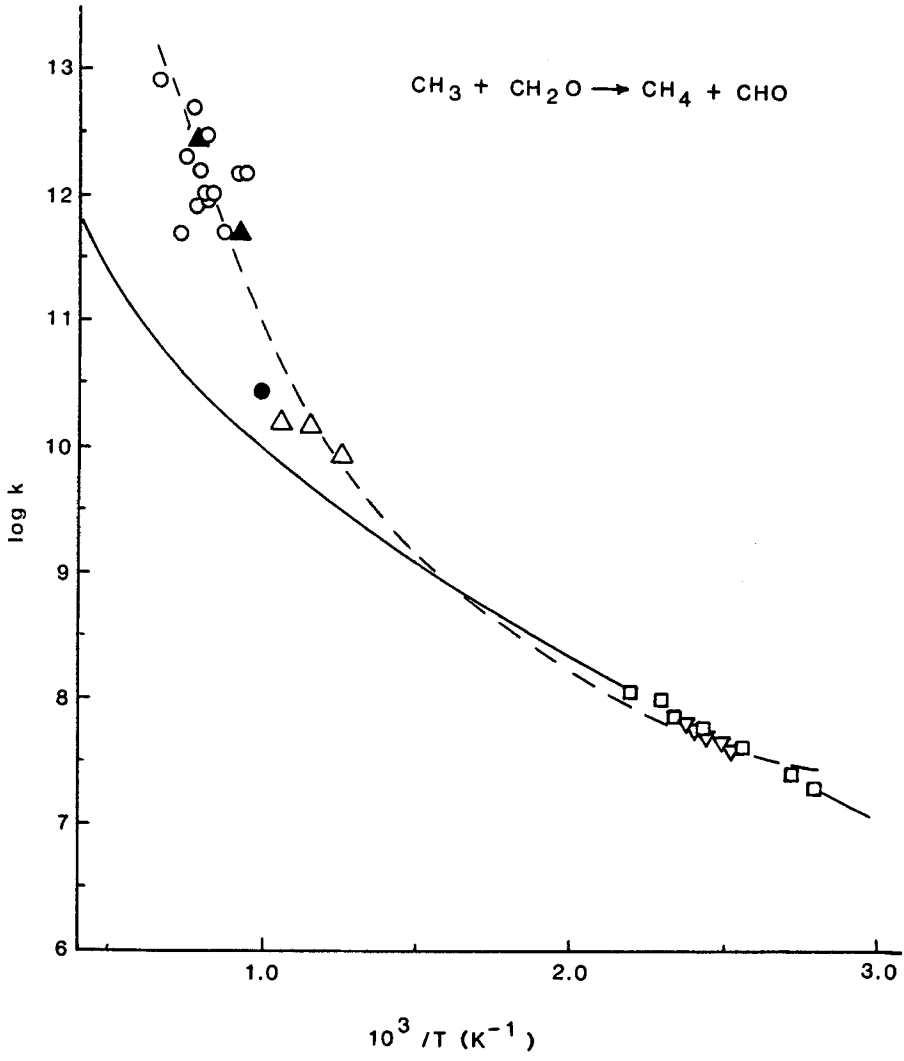

FIGURE A

Arrhenius plots of rate constants for the $CH_3 + CH_2O \rightarrow CH_4 + CHO$ reaction. Open circles are the rate constants extracted from our kinetic modeling. Sources of other data points are : □ , Ref. 37(a); ▽,Ref. 37(b); ●, Ref. 39; △, Ref. 40; ▲, Ref. 41. Dashed curve is from a nonlinear least-squares fit of all experimental points. Solid curve is from our TST calculation. See text.

REFERENCES

1. H.A. Taylor and V.V. Vesselovsky, J. Phys. Chem. 39, 1095 (1935).

2. T.L. Cottrell, T.E. Graham, and T.J. Reid, Trans. Faraday Soc. 47, 584 (1951).

3. L.J. Hildebrand, Jr., and M.L. Kilpatrick, J. Chem. Phys. 19, 381 (1951).

4. Ibid.; J. Chem. Phys. 21, 525 (1953).

5. A. Makovky and T.B. Gruenwald, Trans. Faraday Soc. 55, 952 (1959).

6. A.A. Borisov, S.M. Kogarko, and G.I. Skachkov, Kinetika Kataliz. 7, 589 (1966).

7. K. Glänzer and J. Troe, Helvetica Chimica Acta, 55, 2884 (1972).

8. A. Perche, J.C. Tricot and M. Lucquin, J. Chem. Res. (S) 304, (M) 3219 (1979).

9. D.S.Y. Hsu, W.M. Shaub, M. Blackburn and M.C. Lin, proc. 19th Symp. (Int). Comb., p. 89, The Combustion Institute, Pittsburgh, 1982.

10. D.S.Y. Hsu and M.C. Lin, Proc. of SPIE Symposium, 482, 79 (1984).

11. R.K. Hanson, J.P. Monat and C.H. Kruger, J. Quant, Spectrosc. Radiat. Transfer 16, 705 (1976).

12. D.S.Y. Hsu, G.L. Burks, M.D. Beebe, and M.C. Lin, Int. J. Chem. Kinet., 16, 1139 (1984).

13. S. Gordon and B.J. McBride, NASA SP 273, NASA, Washington, D.C. 1976.

14. T.R. Young and J.P. Boris, J. Phys. Chem., 81, 2424 (1977).

15. F. Westley, "Table of Recommended Rate Constants for Chemical Reactions Occurring in Combustion," NSRDS-NBS 67, National Bureau of Standards, Washington, D.C. 1980.

16. F. Fifer, proc. 17th Symp. (Int.) Combust., p. 567, The Combustion Institute, Pittsburgh, 1978.

17. K.A. Bhaskaran, P. Frank, and Th. Just, "Shock Tubes and Waves," A. Lifshitz and J. Rom, Eds., 1, 503 (1980).

18. D.S.Y. Hsu, W.M. Shaub, T. Creamer, D. Gutman and M.C. Lin, Ber. Bunsenges. Phys. Chem. 87, 909 (1983).

19. These were the rate constant parameters used in Ref. (8). We used these as the high pressure limit parameters for our RRKM calculation and found the calculated results close to being first order.

20. From our thermal RRKM calculations, in which Basco's high pressure limit recombination rate constant (Ref (21)) and Perche's[8] dissociation rate constant were used to obtain the RRKM parameters.

21. N. Basco, D.G.L. James and R.D. Suart, Int. J. Chem. Kinet., II, 215 (1970).

22. Rate constant parameters from Benson and O'Neal (Ref (23)). A thermal RRKM calculation using these as the high pressure limit parameters showed that the calculated rate constant was close to being first order. The model assumed that CH_2NOH, with high-level of excitation from the isomerization step, dissociated into HCN and H_2O via the formation of a tight complex.

23. S.W. Benson and H.E. O'Neal, "Kinetic Data on Gas Phase Unimolecular Reactions," NSRDS-NBS 21, National Bureau of Standards, Washington, D.C., 1970.

24. Calculated using the equilibrium constant and the reverse rate constant. The latter was from D.L. Baulch, D.D. Drysdale, D.G. Horne and A.C. Lloyd, "Evaluated Kinetic Data for High Temperature Reactions," Vol. 2, 1973.

25. Ibid; Vol. 1, 1972.

26. E.G. Schecker and W. Jost, Ber. Bunsenges. Phys. Chem. 73, 521 (1969).

27. D.L. Baulch, D.D. Drysdale and A.C. Lloyd, "Critical Evaluation of Rate Data for Homogeneous Gas-Phase Reactions of Interest in High-Temperature Systems, No. 1, The University of Leeds, 1968.

28. K. Glänzer, M. Quack, and J. Troe, proc. 16th Symposium (Int.) Combust., p. 947, The Combustion Institute, Pittsburgh, 1977.

29. P.D. Pacey and J.H. Purnell, J. Chem. Soc., Faraday Trans. I, 68, 1462 (1972).

30. D.G. Horne and R.G.W. Norrish, Nature 215, 1373 (1967).

31. D.B. Olson and W.C. Gardiner, Combust. Flame 32, 151 (1978).

32. Taken to be same as in the $CH_3 + NO_2 \rightarrow CH_3O + NO$ reaction (Ref. (7)). C_2H_5O is assumed to be unstable and decomposes into CH_3 and CH_2O.

33. A.A. Westenburg and R.M. Fristrom, proc. 10th symposium (Int.) on Combust., 473 (1965).

34. J.A. Fay, J. Chem. Phys. 20, 942 (1952).

35. I.O. Moen, M. Donato, R. Knystautas and J.H. Lee, 18th Symp. (International) on Comb., p. 1615, The Combustion Institute, 1981.

36. R. Guirguis, D. Hsu, D. Bogan and E. Oran, to be published in Combustion and Flame.

37. (a) S. Toby and K.O. Kutschke, Can. J. Chem., 37 672 (1959).

(b) A.R. Blake and K.O. Kutschke, Can. J. Chem., 37, 1462 (1959).

38. J.A. Kerr and M.J. Parsonage, "Evaluated Kinetic Data on Gas Phase Hydrogen Transfer Reactions of Methyl Radicals," p. 150, Butterworths, London, 1976.

39. A.M. Held, K.C. Manthorne, P.D. Pacey and H.P Reinholdt, Can. J. Chem. 55 4128 (1977).

40. K.C. Manthorne and P.D. Pacey, Can. J. Chem. 56, 1307 (1978).

41. D. Aronowitz and D. Naegeli, Int. J. Chem. Kinet. 9, 471 (1977).

42. M.T.H. Liu and K.J. Laidler, Can. J. Chem. 46, 479 (1968).